Journal of Information Systems and Telecommunication
Vol.11, No.4, October-December 2023, 269-281
http://jist.acecr.org
ISSN 2322-1437 / EISSN:2345-2773

Implementation of Uplink and Downlink Non-Orthogonal Multiple Access (NOMA) on Zync FPGA Device

Ahmed Belhani[1*], Hichem Semira[2], Rania. Kheddara[1], Ghada Hassis[3]

[1].Laboratoire Satellites, Intelligence Artificielle, Cryptographie, Internet des Objets « LSIACIO», Constantine 1 University, Algeria
[2].Electronics and New Technologies Laboratory (ENT), University of Oum El Bouaghi, Algeria
[3].Department of Electronics », Constantine 1 University, Algeria.

Received: 24 Jan 2022/ Revised: 04 Sep 2022/ Accepted: 02 Oct 2022

Abstract

The non-orthogonal access schemes are one of the multiple access techniques that are candidates to become an access technique for the next generation access radio. Power-domain non-orthogonal multiple-access (NOMA) is among these promising technologies. Improving the network capacity by providing massive connectivity through sharing the same spectral resources is the main advantage that this technique offers. The NOMA technique consists of exploiting the power domain which multiplex multiple users on the same resources applying a superposition coding then separating the multiplexed users at the receiver side. Due to the non-orthogonality access technique, the main disadvantage of NOMA is the presence of interferences between users. That is why this scheme is based on a successive interference cancelation (SIC) detector that separates the multiplexed signals at the receiver. In this paper, an embedded system is considered for designing and implementation of the power-NOMA For two users. The implementation is realized by employing a Zynq FPGA (Field programmable gate array) device through the Zybo-Z7 board using MATLAB/Simulink environment and Xilinx System Generator. The features offered by this device, hemps to consider the design of an uplink and a downlink scenario over Rayleigh fading channel in additive white Gaussian noise (AWGN) environment.

Keywords: Non-Orthogonal Multiple Access (NOMA); Successive Interference Cancelation (SIC); Multi-use Detection; Bit Error Rate (BER); QPSK; BPSK; Xilinx System Generator (XSG.

1- Introduction

The phenomenal development in communication systems and Internet of Things (IoT) has increased the demand for better internet connections, higher data rates, less latency, fairness, better Quality of Service (QoS), and reduced interference [1][2].

Communication networks in the next generation (5G and beyond) aspire to achieve high efficiency [2], through more users in the limited available spectrum [1]–[5] by applying a new Medium Access Control (MAC) called NOMA technique[5]. In recent years, NOMA-IoT has attracted many researchers in academia [5]–[8]. This growing interest is due to the fact that the NOMA technique is a good candidate to address some of the challenges regarding the radio spectrum scarcity. Dealing with this shortage is one of the challenges to ensure a massive machine-type communication (MMTC) (e.g., IoT framework) by attaining ultra-low latency and high reliability.

The conventional technique OMA (Orthogonal multiple access) permits multiple access by limiting the number of users to the number of available resources based on the orthogonality between users [5], Some of these techniques are, time division multiple access (TDMA), frequency division multiple access (FDMA), and code division multiple access (CDMA)[9]. These techniques are the reasons why the OMA scheme cannot meet the demands of concurrent users due to the resource shortage, especially against the increasing number of connected devices in the IoT network [10]. Contrarily, NOMA uses the same frequency block and the same time slot by assigning different power levels or by multiplexing signals in code domain [1][2], which helps to enhance the bandwidth reuse and connectivity density [6].

✉ **Ahmed BELHANI**
ahmed.belhani@umc.edu.dz

While OMA systems use orthogonal resource allocation among users to avoid interference [1], the NOMA technique intentionally introduces interference because of its principle of access and superposition of users' data. Consequently, the successive interference cancellation (SIC) technique has been widely adopted in the NOMA literature as a solution to eliminate the inter-user interference. In SIC, the first step consists of estimating the strongest signal by treating other superposed signals as noise. In the second step, the decoded signal is subtracted from the received signal to retrieve the weakest signal [8].

From an information theoretic viewpoint, the fundamental potential of NOMA over OMA has been proved. Indeed, most of the analytical studies handled in terms of information-theoretical perspectives, have revealed the efficiency of the SIC detector in both schemes uplink-NOMA and downlink-NOMA e.g. [11]–[13]. These analyzes are based on the SINR (Signal to Interference and Noise Ratio) definition and then they provide theoretical limits for throughput or outage probability. However, in throughput or outage analysis the SIC algorithm is not implemented. Therefore, the analysis could only give inferences for theoretical limits. In other words, the NOMA system with its transmitter and receiver (SIC algorithm) is not implemented or simulated while assuming perfect SIC. Hence, in real world application, to analyze the error performance of the NOMA schemes (in terms of bit error rate BER), we should implement an IQ (in-phase and quadrature inputs) modulator at the transmitters and based on the superimposed received signal, we should implement an IQ detector to decide the transmitted symbols (bits) of each user. This implementation could give us a clear idea about the imperfections of the detection technique (i.e. subtraction of the erroneous detected symbol) [13]

To study the efficiency of the SIC receiver, a practical downlink-NOMA system based on LTE specifications using an open-source software platform named Open Air Interface have been investigated in[3]. The experiment results of the work demonstrate that the NOMA scheme has a significant throughput gain compared with an orthogonal multiple access (OMA) scheme.

Currently, the use of FPGAs in research and development of embedded systems is applied to specific tasks is increasing [15], for many valuable advantages such as its great flexibility [15], which allows the re-use of any circuit as desired in different structures in a very fast time, high clock frequency, high operations per second, and parallel processing [15]. FPGAs are widely used in the communication field to benefits their capacity, function and reliability [16] such as the space-time coding and decoding algorithms for MIMO Communication system presented in [17], and the FPGA implementation of a Pseudo Chaos-signal generator for secure communication systems in [18].

In addition, the implementation of differential frequency hopping communication system is studied in [19]. In [20], NOMA technique is experimentally investigated over AWGN channel using FPGA. The authors propose an implementation based on VHDL programming for two users in the downlink scenario. In addition to the design of the transmitter and the SIC in receiver, the authors relied on a Box-Muller method for noise generation. Furthermore, the performance is verified by comparing the Monte-Carlo simulation results via MATLAB showing exact matching with that of the designed NOMA system. However, this study is only limited to the downlink scheme over AWGN environment which is not reasonable for practical situation, where the channel coefficients are consistently present to affect the received signal (path loss, fading and shadowing). In this paper, we propose the implementation on FPGA of a real-time transmission concept of the power domain NOMA for both scenarios: downlink and uplink over Raleigh fading channel. At first, derived from Monte-Carlo simulation via MATLAB, we study the performance of power NOMA technique in both schemes using QPSK and BPSK modulation. Hence, for proper implementation and avoiding overlap between the users' symbols, the power allocation principle is assured for the downlink scheme, on the other hand, we keep the uplink scheme without scheduling of power allocation as the users use their own power.

Afterwards, with the assumption of two users like the work of [20], and based on Xilinx system generator (XSG) which is a high-level design tool that allows the use of the MATLAB / Simulink environment, we design the functional blocs for an implementation of the power NOMA technique on the FPGA Zybo Z7 card for both schemes (downlink and uplink). This implementation is made simple by using Xilinx library to create elements allowing FPGA hardware design without resorting to HDL programming [21].

The rest of the paper is organized as follows. Section 2 presents some assumptions used in the work, while section 3 illustrates the system and the channel models. section 4 shows the simulation results obtained for both link: downlink and uplink over Rayleigh fading channels and AWGN. In section 5, we describe the FPGA card used in the work and the waveforms of the system generator models with the RTL schemes. Finally, a conclusion is presented in section6.

2- Assumptions

In this work, we assume the presence of two users in the network, this assumption is due to the fact that regardless

of the number of users, the remote user always considers other users signals as just additive noise as defined by NOMA theory [20]. Moreover, we assume that the power allocation factors a_N and a_F used for the two users are known, and that the path is non-selective.

In the uplink scenario, the base station is free of scheduling the power allocation as long as each user uses and manages its own battery. Hence, we assume that each user uses its own battery power to the maximum with a factor equal to 1.

3- NOMA Model

This section presents the NOMA model in power domain for both links.

3-1- Downlink NOMA

In a downlink scheme shown in Figure 1, we consider two users equipped with one antenna served by a base station (BS) equipped with a single transmitting antenna (Single Input Single Output (SISO)). The BS transmits with power P the signals of users superposed on the same resource block. The superposition is realized at the BS by adding the different symbols after power scaling both symbols are combined using superposition coding principle (SC); the more power is allocated to the far user (FU); the less power allocation ratio is allocated to the near user (NU), i.e., the information for both users is multiplexed in the BS using the same resource block (frequency/time) by allocating each user a different power coefficient by virtue of its channel conditions. The power allocation ensures fairness for all users by maintaining a specific BER thresholds for each user [22]. Hence, the signals $y_k \in \mathbb{C}$, $k \in (F, N)$, received by users are described as shown by Eq. (1):

$$y_k = h_k\left(\sqrt{a_F P}s_F + \sqrt{a_N P}s_N\right) + n_k, \quad k \in (F, N), \tag{1}$$

where h_k denotes the flat fading channel coefficients between the BS and the kth user, i.e. $k \in (F, N)$. The independent and non-identical Rayleigh fading channel coefficients h_k, $k \in (F, N)$ are modeled as complex Gaussian random variables with zero mean and variance $E[|h_k|^2]$, i.e., $h_k \sim CN(0, E[|h_k|^2])$, $k \in (F, N)$, where $|.|$ denotes the absolute value and $E[.]$ is statistical expectation. At each kth user the channel coefficients h_k, $k \in (F, N)$ is supposed to be known, such that $|h_F| < |h_N|$. As a consequence, the power allocation factors a_N and a_F are assigned such that $a_N < a_F$, where $a_F + a_N = 1$. $n_k \sim CN(0, N_0/2)$, $k \in (F, N)$, is the additive white Gaussian noise (AWGN) which is added at each node (each user's receiver) independently.

The information bits are modulated as complex symbols s_F, s_N using a phase modulated signals for both users, they can be a QPSK modulation signals which can take four possible complex values defined as $s_k = \pm 1 \pm j1$, $k \in (F, N)$, resulting from the mapping of two bits, or a BPSK modulation signals which can take one of the two possible symbols ± 1.

In the network, all users receive the same signal, which contains the information of all users. This requires a suitable detector to eliminate interference in each equipment. Since a large part of the power has been allocated to the FU, a maximum likelihood detector (MLD) is sufficient to detect the information of this user by considering the signal of the NU as interference. On the other hand, the NU must first detect the interference signal (FU) as its own symbol is noise. In the second step, it removes the detected symbol from the received signal y_N in order to detect its own symbol. This procedure is known as successive interference cancelation (SIC), and it is clear that the performance of the system depends on the channel qualities and the power allocation coefficients [13]

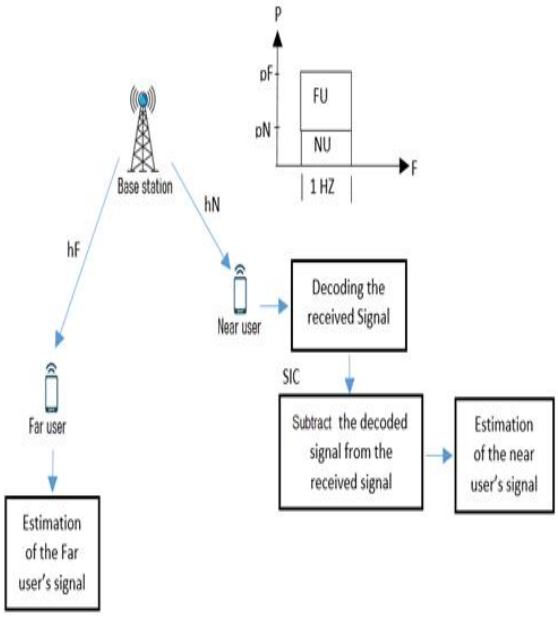

Fig. 1 Downlink Power Domain NOMA for Two Users with SIC Technique.

3-2- Uplink NOMA

As shown in Figure 2, Similar to the downlink scenario, the uplink scheme is composed of one base station and two users. Even in this scenario, we assume that each node is equipped with a single antenna (SISO-NOMA). With transmit power P_k, $k \in (F, N)$, limited by the

maximum power of the user battery, each user can independently use its own power P_k to transmit its symbols on the same frequency block within the same time slot. Therefore, the received signal $y \in \mathbb{C}$ at the BS is given by Eq. (2):

$$y = h_N\sqrt{P_N}s_N + h_F\sqrt{P_F}s_F + n \qquad (2)$$

where the Rayleigh fading channel coefficients $h_{k,}$ $k \in (F, N)$, between the users and BS are independent and identically distributed. s_N and s_F are the complex modulated information from QPSK or BPSK modulation. n denotes the AWGN at BS receiver. Like the downlink. scenario it is assumed that $\sqrt{P_F}\ |h_F| < \sqrt{P_N}|h_N|$. By virtue of the quality of the channel and the level of received power, firstly, the BS attempts to detect the symbols of the NU using MLD by considering the signal received from the FU ($h_F\sqrt{P_F}s_F$) as noise. Secondly, after having removed the detected symbol ($h_N\sqrt{P_N}\hat{s}_N$, where $\hat{s}_N$ denotes detected s_N), the BS attempts to detect the symbols $\hat{s}_F$ using MLD

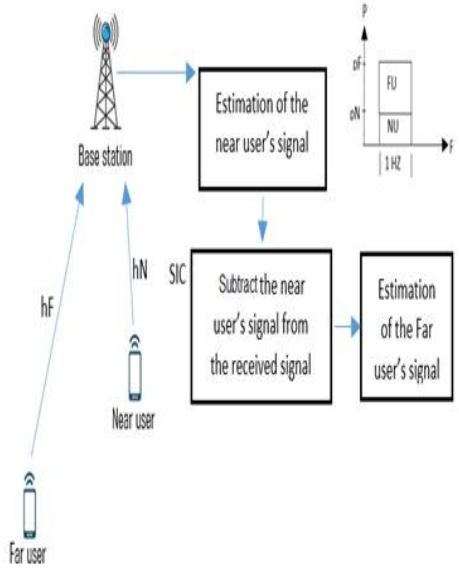

Fig. 2 Uplink Power Domain NOMA for Two Users with SIC Technique.

4- Simulation and Main Results

4-1- Downlink

Figue 3 shows the flowchart of the downlink-NOMA system. Firstly, we generate a random data for both users then we modulate them using either a QPSK modulation or a BPSK modulation, after, we multiply the two signals by the power allocation factors a_N and a_F.

In the next step, we combine the two signals to construct the NOMA signal x_{NOMA} multiplied by the Rayleigh coefficients for each user, and then we start the estimation process after adding the white noise for each user separately.

The FU estimates its data directly from the received signal via a minimum-distance criterion (MLD), whereas the NU utilizes the SIC technique to obtain its symbols.

To illustrate the performance of the NOMA system in the downlink scheme, we use the parameters presented in the table1.

Table 1: Simulation Parameters

Monte Carlo runs		10000
Power allocation factors for the near user		0.2, 0.4
Power allocation factors for the far user		0.6, 0.8
System frequency		15360000 Hz
Rayleigh Channel parameters	Path Delays	0 S
	Average Path Gains	FU: -3 dB
		NU: 0 dB
	Maximum Doppler Shift	0 HZ

Figures 4, 5 and 6 show the simulation results for the bit error rate (BER) against the Signal to Noise ratio per bit (Eb / No) for different scenarios. In figure 4, we consider a QPSK modulation for both users with different power allocation. We can easily observe the influence of the power allocation coefficients on the performance of the system. The more the symbols of the different users are well separated in power, the more we prevent the constellations overlap of different users. Furthermore, the curves show that the BER of FU is better than that of NU for $a_N = 0.2$ and $a_F = 0.8$, which shows the compensation of the effect of the channel with the enhancement of the symbols power for the FU.

In the second scenario in which the same power allocation factors are maintained, we consider two cases of modulation: Fixed QPSK modulation for both users, and adaptive modulation for the second case. In adaptive modulation, a BPSK modulation is chosen for the FU which suffers from the worst channel condition, and a QPSK modulation is used by the NU which benefits from high channel quality. For different power allocation factors, the Figures 5 and 6 show clearly the improvement of the BER for the adaptive modulation compared to the fixed modulation. In addition to avoiding overlap between the symbols of different users, the low order modulation compensates the effect of the channel by increasing the power of the symbols and also by helping the detection threshold to be improved when using the MLD for both users.

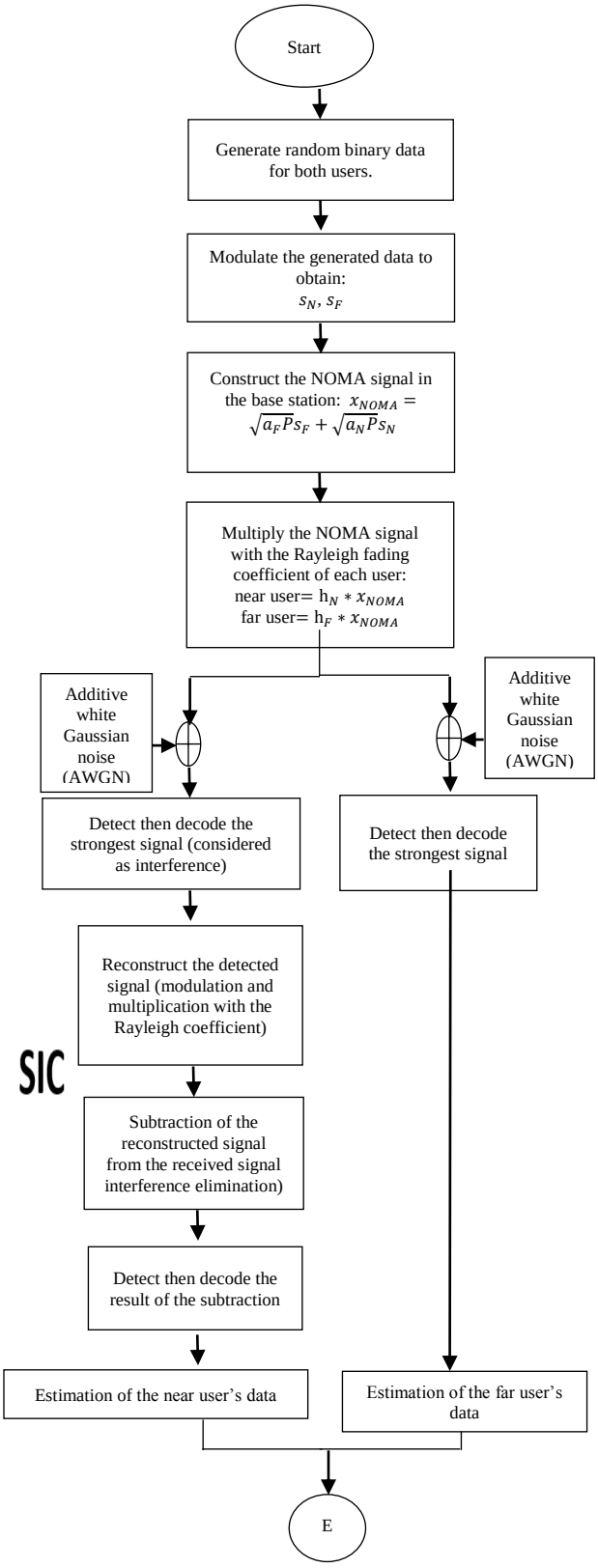

Fig. 3 Flowchart of the Downlink NOMA.

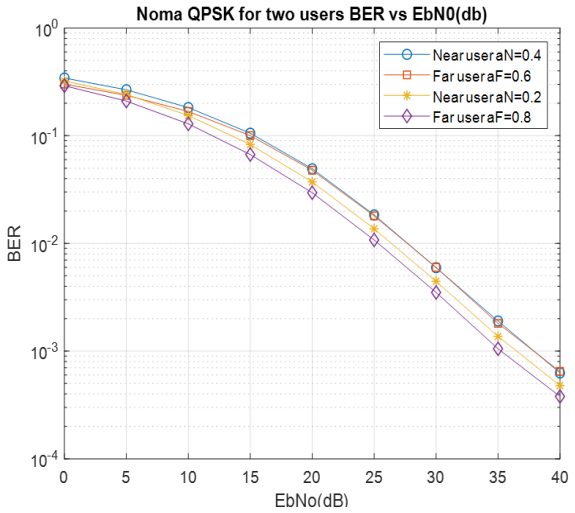

Fig. 4 BER vs E_bN_0 for the Downlink Power Domain NOMA Transmission Using the QPSK Modulation and the Power Allocation Factors of a_N = 0.2, 0.4, a_F = 0.6, 0.8.

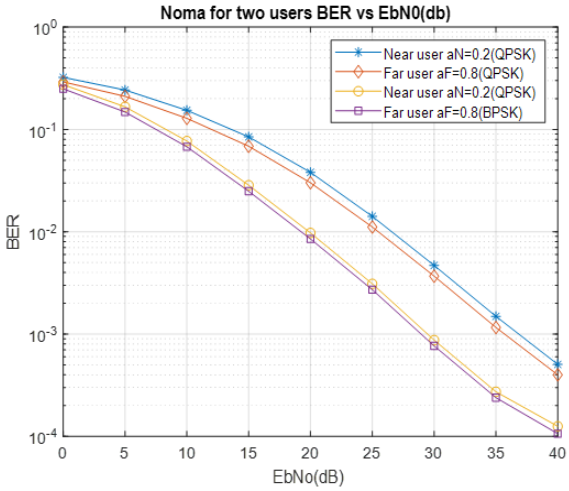

Fig. 5 BER vs E_bN_0 for the Downlink Power Domain NOMA Using the QPSK Modulation and the Power Allocation Factors of a_N = 0.2, a_F = 0.8.

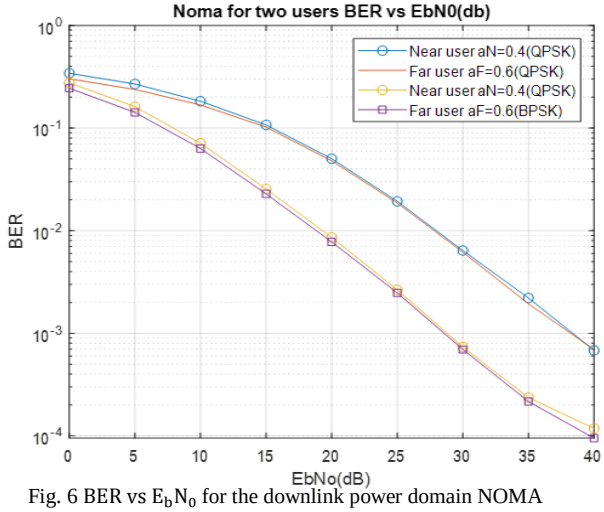

Fig. 6 BER vs E_bN_0 for the downlink power domain NOMA Transmission Using the QPSK and the BPSK Modulations and the Power Allocation Factors of a_N = 0.4, a_F= 0.6.

4-2- Uplink

Figure 7 shows the flowchart of the uplink–NOMA system. Like the previous scheme, we randomly generate the binary data for each user then we modulate them by using either a QPSK modulation or a BPSK modulation according to the channel quality. Unlike the previous diagram, in the uplink-NOMA scheme, each user sends its own data using its own power (power battery) toward the BS, which results in multiplication by independent Rayleigh coefficients and power. In consequence, the two signals are firstly multiplied by different Rayleigh coefficient (h_N for the NU and h_F for the FU) and Powers (P_N for the NU and P_F for the FU) according to their distance from the base station and their own battery. After that, the signals are multiplexed at the BS. Finally, the estimation process begins after the white noise is added.

The base station estimates the NU data directly through the ML detector by considering the FU data as noise. In the next step, the BS tries to detect the far user's symbols via MLD after subtracting the detected signal (previous step) from the received signal.

To illustrate the behavior of the SIC algorithm with the performance of the uplink-NOMA scheme, we adopt the same simulation parameters of the downlink-NOMA scheme. The figures 8 and 9 show the performance of the BER versus EbN0 in the uplink-NOMA system for two types of modulations QPSK and BPSK. To show the performance, we present two scenarios: fixed modulation and adaptive modulation in proportion to the quality of the channel. In all the simulation, we assume that $P_N = P_F$, which reflects a practical situation where the two users transmit with the same power like the IoT devices.

It can be seen from the two figures that the performance of the FU is better than the performance of Nu in terms of BER. This superiority is due to the use of SIC detector at the base station to estimate the FU's data, which suppresses the strong signal assumed to be interference. On the other hand, the base station only uses the maximum likelihood detector to extract the NU's data, which suffers from the presence of FU'S symbols considered as noise. Despite these results, we can notice from all the curves in uplink-NOMA scheme that the SIC presents a poorer performance in high SNR regime and clearly suffers from the error floor [13][23][24]. According to the figures 8 and 9, we observe that increasing the transmit power (high SNR) or using low order modulation (BPSK) at the receiver cannot remove the error floor. Indeed, whatever the improvements, the SIC detector remains unable to detect the symbols of the different users in a high SNR regime, which is an inevitable result because other signals are treated in a sequential manner on the basis that they are noise.

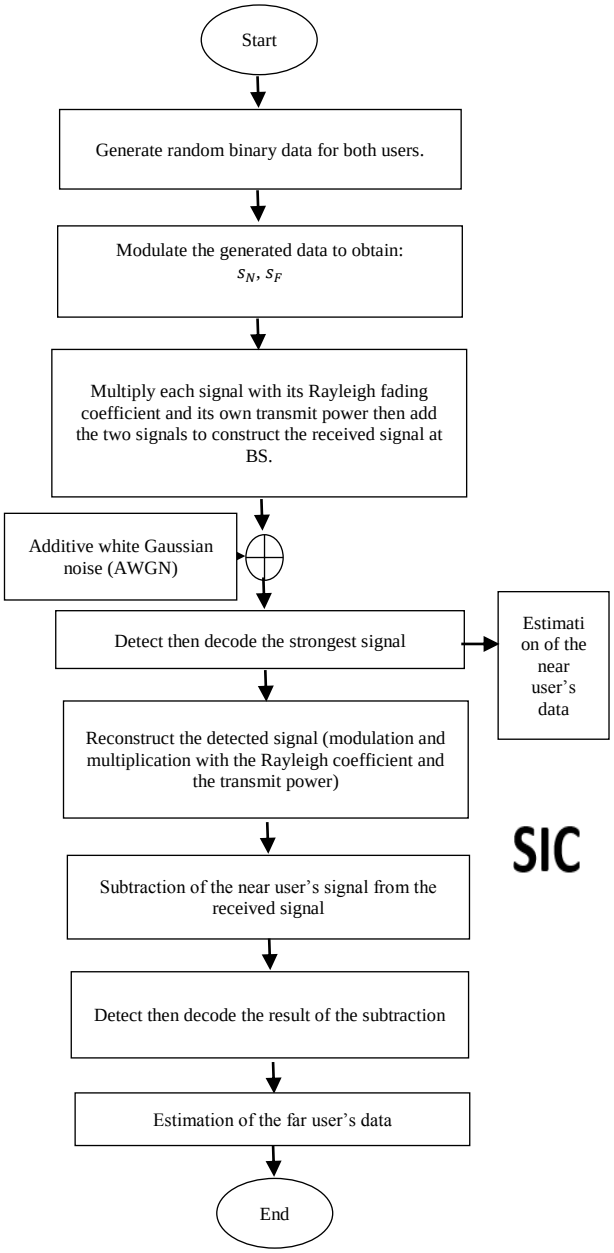

Fig. 7 Flowchart of the Uplink NOMA.

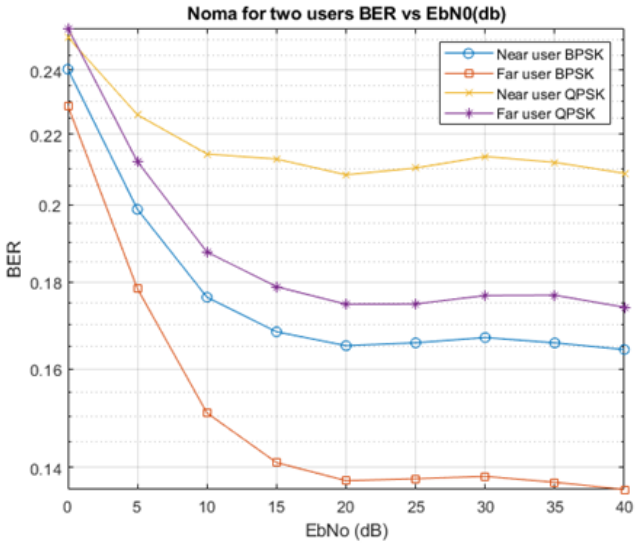

Fig. 8 BER vs E_bN_0 for the Uplink power domain. NOMA Transmission With the Using the Same Modulation for Both Users QPSK or BPSK Modulation.

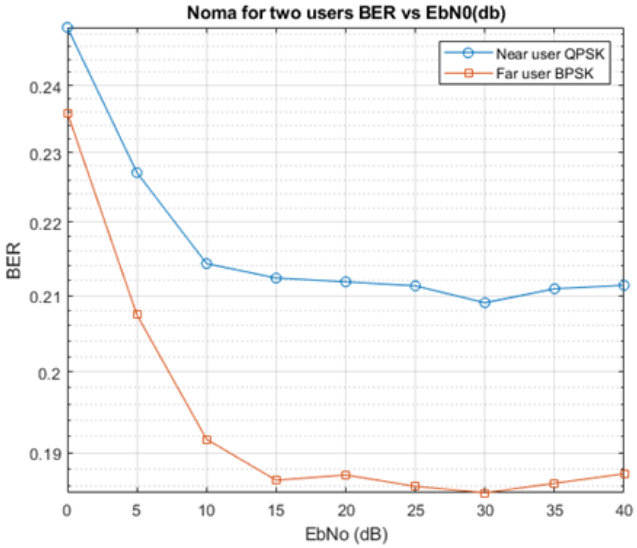

Fig. 9 BER vs E_bN_0 for the Uplink Power Domain. NOMA Transmission Using the QPSK Modulation for the NU and the BPSK Modulation for the FU.

5- Implementation of NOMA Models Using System Generator and ZYBO-Z7 Xilinx Card

In this section a Zybo Z7 card based on Zynq-7020 device is used to implement the power domain NOMA technique for both schemes: downlink and uplink. This choice is based on its features and connectivity [15] illustrated by table 2. The power tool system generator of Xilinx is combined with Matlab/Simulink to design the NOMA signal and build VHDL project, which is transferred to VIVDAO suite for waveform generation through test bench

Table 2: Zybo-Z7 Characteristics

ZYBO Z7 features	ZYBO Z7 specifications	ZYBO Z7 connectivity
667MHz dual-core Cortex-A9 processor with tightly integrated Xilinx FPGA	Clock Resources Zynq PLL with 4 outputs 4 PLLs (2 PLLs*) 4 MMCMs (2 MMCMs*) 125 MHz external clock	Wide range of USB, Ethernet
High-bandwidth peripheral controllers: 1G Ethernet, USB 2.0, SDIO)	Block RAM:630 KB (270 KB*)	Pcam camera connector
Programmable from JTAG, Quad-SPI flash, and microSD card	Internal ADC Dual-channel	HDMI sink port (input)
DDR3L memory controller with 8 DMA channels and 4 High Performance AXI3 Slave ports	DSP Slices :220 (80*)	6 Pmod ports (5*) :8 Total Processor I/O ,40 Total FPGA I/O (32*) , 4 Analog capable - 1.0V differential pairs to XADC

5-1- Downlink Implementation

Figure 10 shows the NOMA design using Xilinx system generator tools for the downlink, contains: The BPSK modulator, the BSPK demodulator, the transmitted NOMA signal, the received Far user signal and the received near user signal. We have also maintained the same parameters shown in table 1

5-2- BPSK Modulator/Demodulator

The logic elements are used to build all components, like multiplexer, multiplier, adder and delay element.
Figure 11 shows the BPSK modulator designed through XSC tools [25].
For the BPSK demodulator, we use the structure defined in [26] and accomplished it by adding a low pass filter design with eleven coefficients presented in table 3 to get more precision. Figure 12 shows the demodulator released through the DSP's FDA tool from XSG toolbox

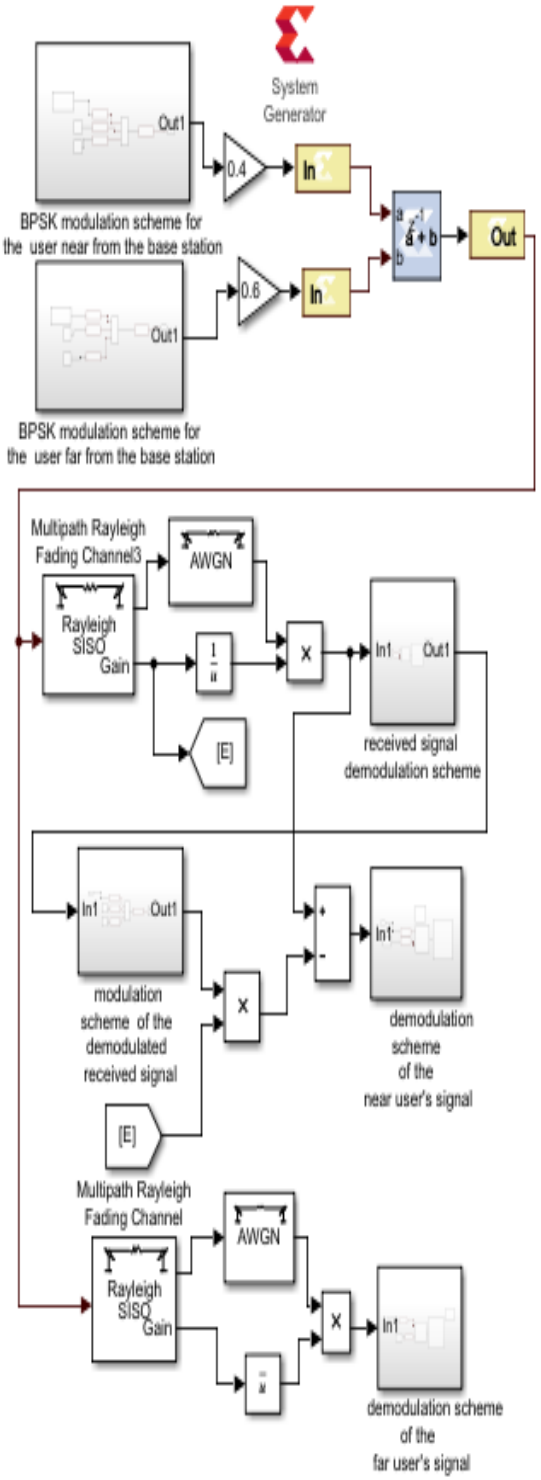

Fig. 10 NOMA Design for the Downlink Using Systems Generator and Xilinx Tools.

Table 3: Low Pass Filter CoefficientS

Coefficient number	coefficient value	Coefficient number	coefficient value
1	-0.0732	7	0.1763
2	0.1712	8	0.1601
3	0.1469	9	0.1469
4	0.1601	10	0.1712
5	0.1763	11	-0.0732

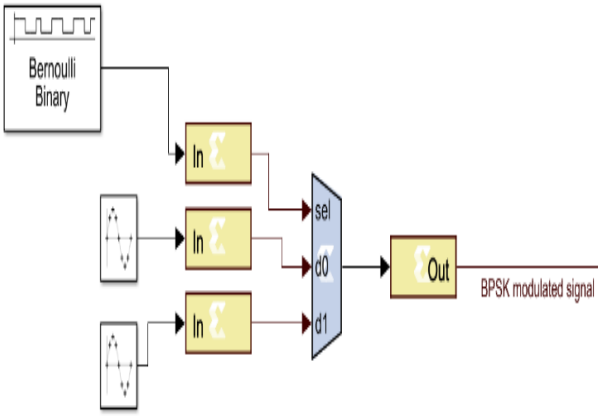

Fig. 11 BPSK Modulator.

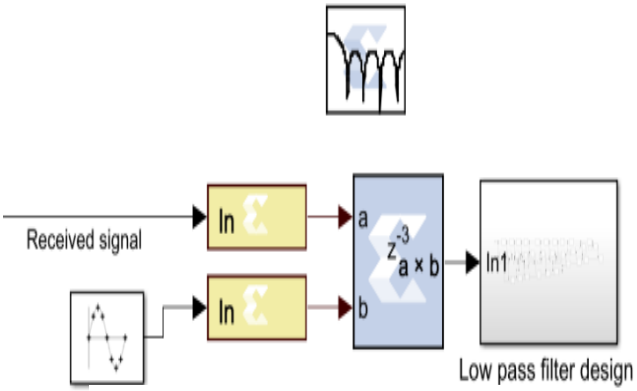

Fig. 12 BPSK Demodulator

Figures 13 and 14 show clearly the BPSK modulator and demodulator waveforms for the designed models in the downlink. The choice of using a BPSK modulation in the XSG model is only to simplify the design and the results; we can use any type of modulation, for example QPSK modulation[20].

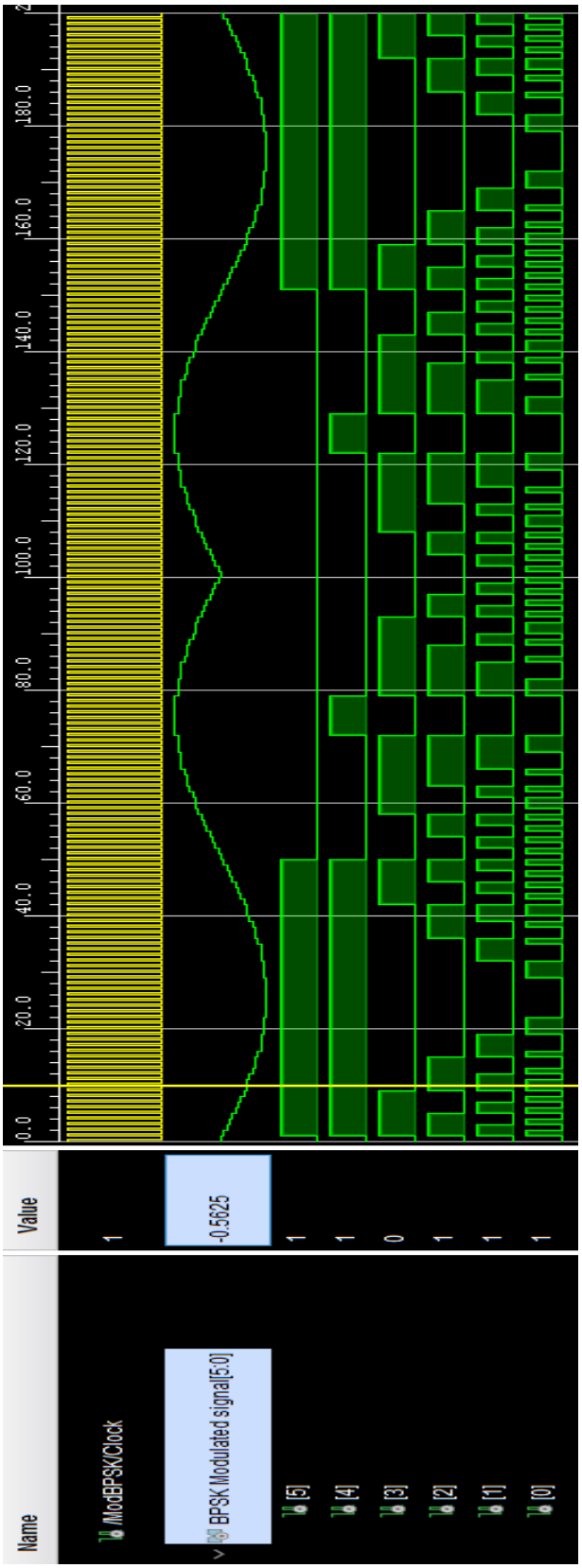

Fig. 13 BPSK Modulator Waveform

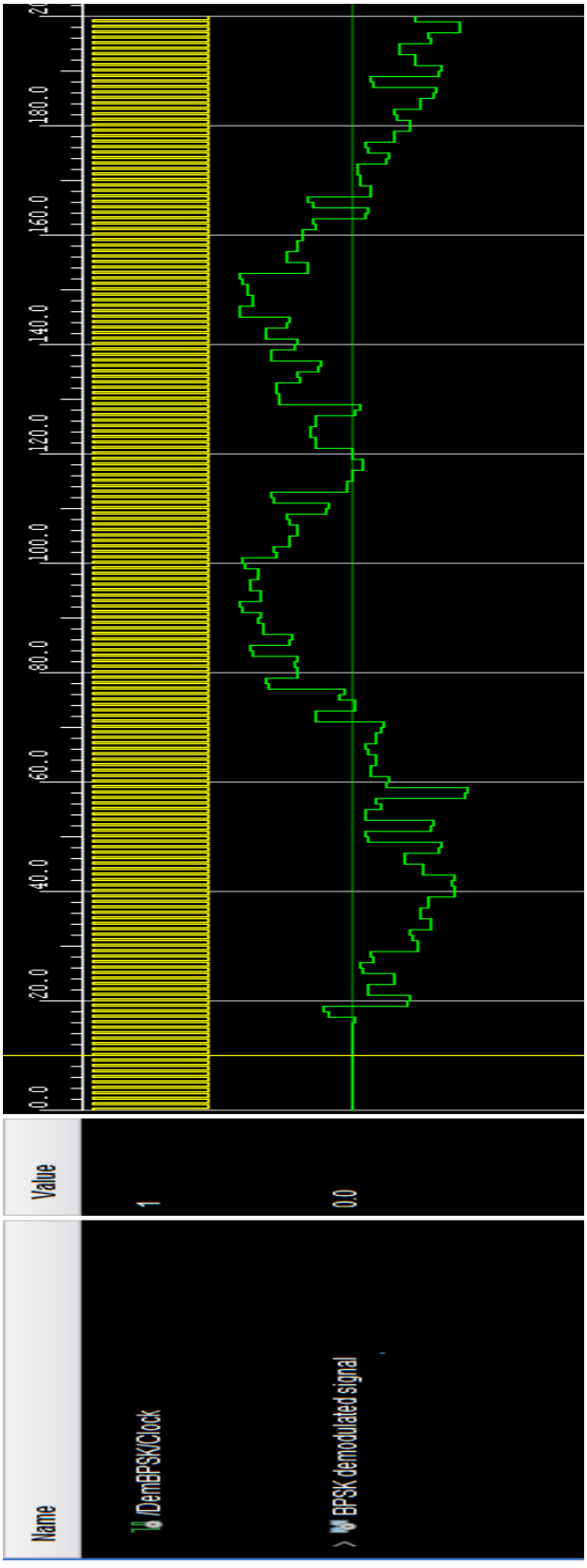

Fig. 14 BPSK Demodulator Waveform

5.2.1 NOMA Signal

Figure 15 represents the NOMA signal design for the downlink, where we multiply the BPSK modulated signal of each user with the power allocation factors, and we combine the two signals to obtain the NOMA signal, the result of the waveform is illustrated in figure 18.

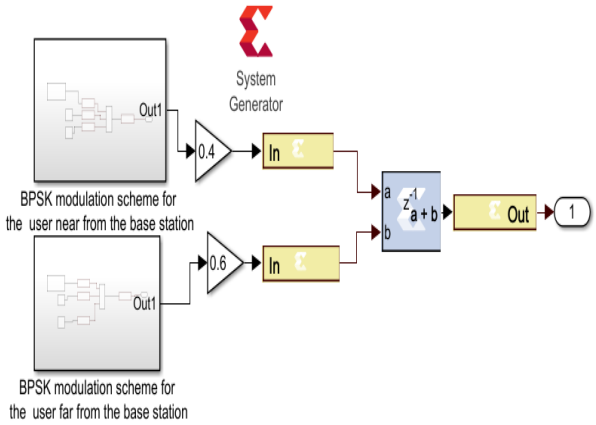

Fig. 15 NOMA Bloc Design for Downlink.

5.2.2 Far User and Near User

Figures 16 and 17 represent the two designs for the estimation process mentioned above and explained in the flowchart of the downlink. In the other hand, for the far user we implement the SIC technique to estimate the near user's signal (figure17).
In figure 18, we directly demodulate the far user's signal after passing through Rayleigh fading channel and AWGN.

5-3- Uplink Implementation

Figure 19 shows the NOMA design using Xilinx system generator tools for the uplink, which contains the same blocks used in the downlink.

5.3.1 NOMA Signal

Figure 20 represents the NOMA signal design for the uplink, which contains the two users BPSK modulated signals and the Rayleigh fading channels for each user combined and passed through Rayleigh and AWGN channel.

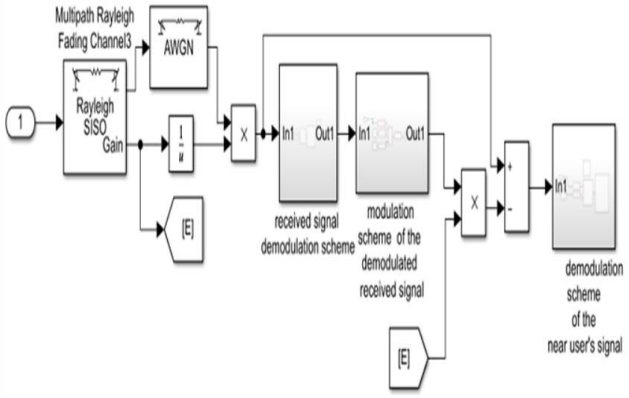

Fig. 17 Near User Reception Design for Downlink.

5.3.2 Far User and Near User

Figures 21 and 22 represent the two designs for the estimation process mentioned above and explained in the flowchart of the uplink; we first estimate the near user's signal in figure 21, afterwards, the far user's symbols are detected using SIC procedure using the same received signal as the SIC is implemented in BS.

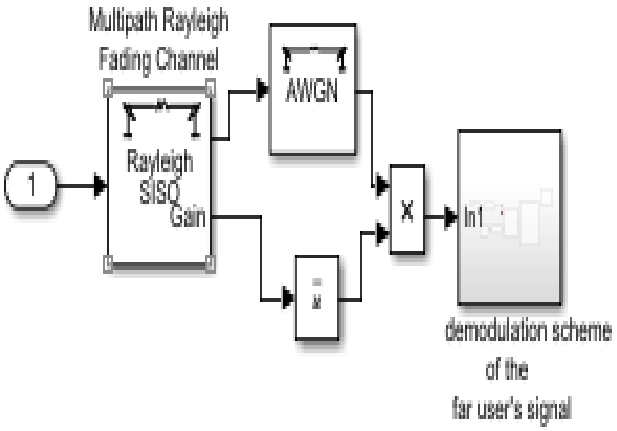

Fig. 16 Far User Reception Design for Downlink.

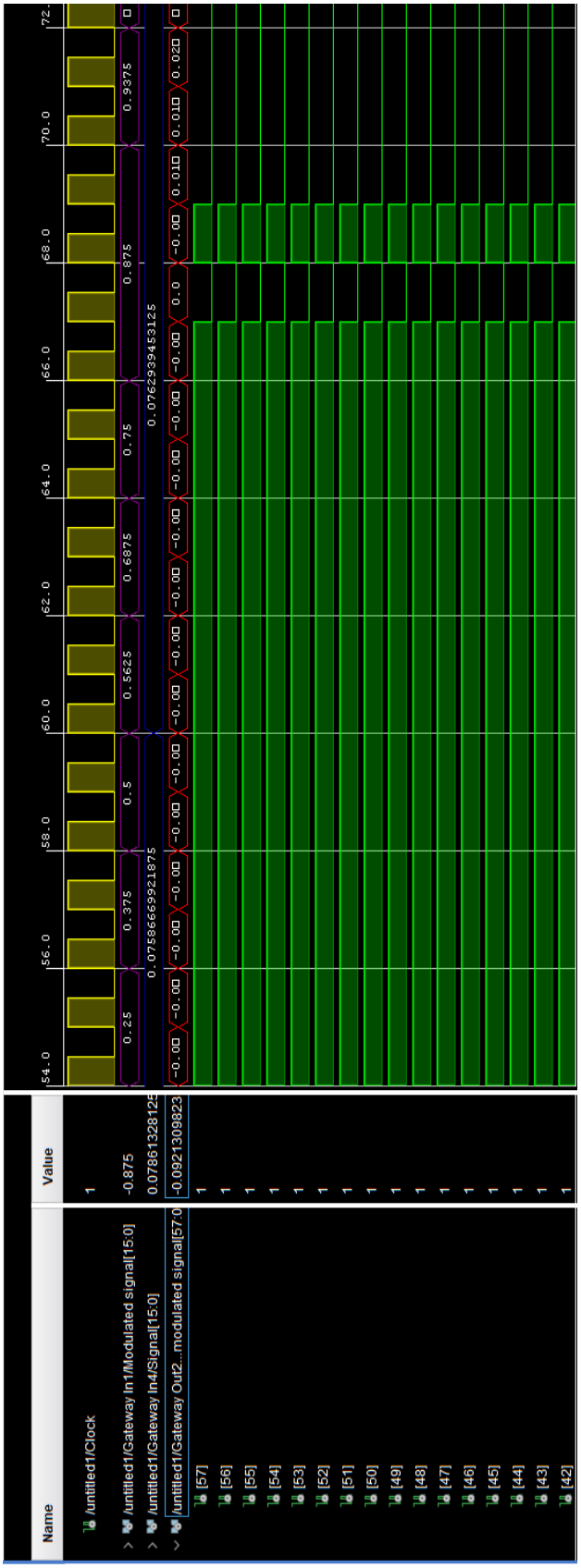

Fig. 18 NOMA Signal Waveform for the Downlink

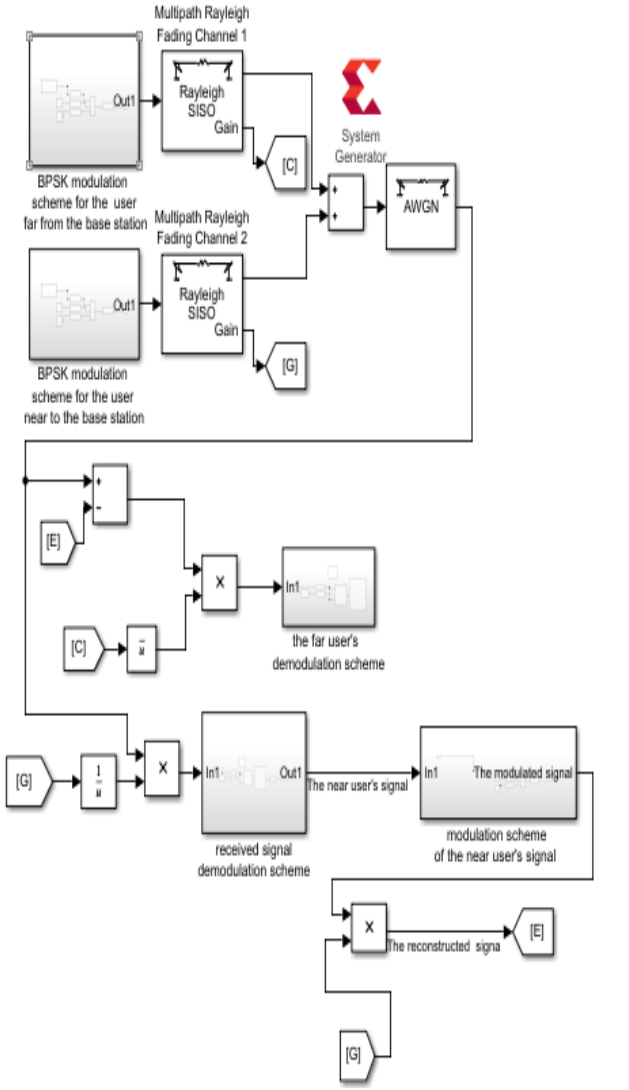

Fig. 19 NOMA Design for the Uplink Using Systems Generator and Xilinx Tools.

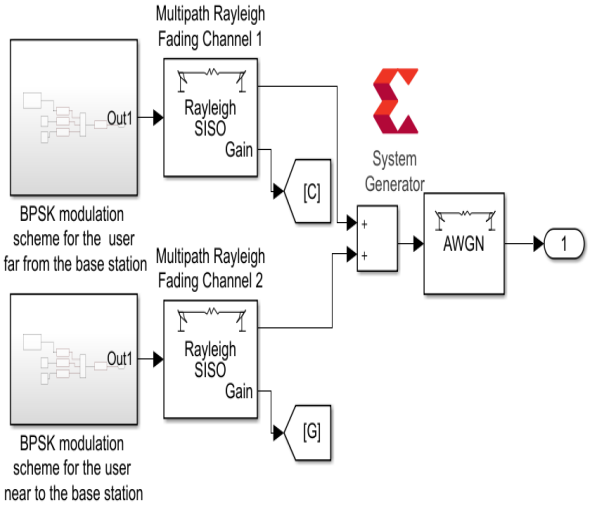

Fig. 20 NOMA Design for Uplink.

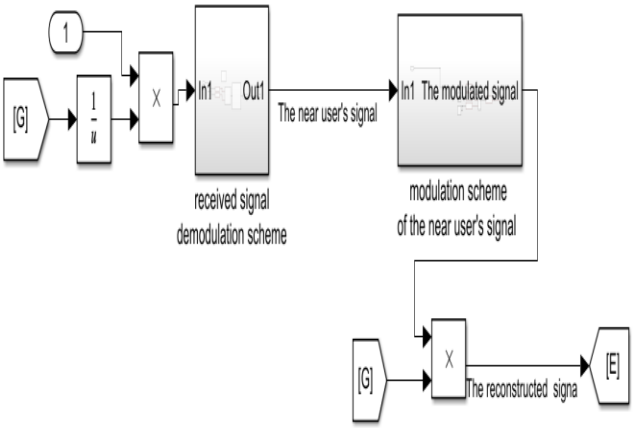

Fig. 22 Near User Reception Design for Uplink.

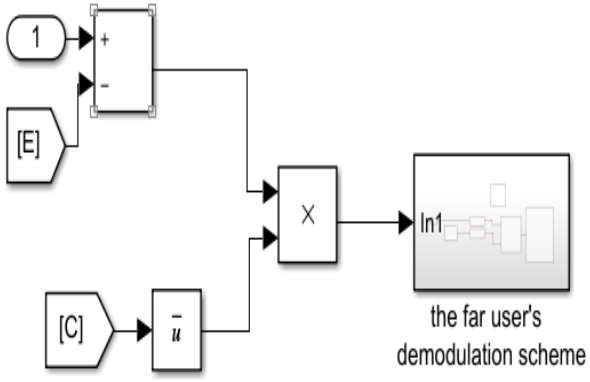

Fig. 21 Far User Reception Design for Uplink.

6- Conclusion

In this paper, the power NOMA technique in uplink and downlink links are studied and implemented on an FPGA device. The implementation is realized for two users supported by one base station over Rayleigh fading channel. In both schemes a successive interference cancelation (SIC) detector is considered in the receiver side to separate the superimposed symbols of users. The Conclusion
simulation results reveal the effectiveness of the SIC algorithm to detect the user's symbols in downlink link by using both modulation: QPSK or BPSK. By contrast, in the uplink scenario where there is no scheduling of power allocation, the SIC fails to detect any symbols in high SNR regime (suffers from the error floor). Besides, to benefit from the advantages offered by the features of the FPGA device, a design of both schemes is realized using the Xilinx system generator. The results of this work may be extended to address the implementation of this promising technique to deal with a massive connection (arbitrary number of users with higher order adaptive modulation) for IoT applications

Acknowledgement.

The authors thank Dr Cherif chibane from MIT for his help.

References

[1] L. Dai, B. Wang, Y. Yuan, S. Han, I. Chih-lin, et Z. Wang, « Non-orthogonal multiple access for 5G: solutions, challenges, opportunities, and future research trends », IEEE Commun. Mag., vol. 53, no 9, p. 74‑81, sept. 2015.

[2] M. Moltafet, N. Mokari, M. R. Javan, H. Saeedi, et H. Pishro-Nik, « A New Multiple Access Technique for 5G: Power Domain Sparse Code Multiple Access (PSMA) », IEEE Access, vol. 6, p. 747‑759, 2018.

[3] X. Wei et al., « Software Defined Radio Implementation of a Non-Orthogonal Multiple Access System Towards 5G », IEEE Access, vol. 4, p. 9604‑9613, 2016.

[4] Z. Ding et al., « Application of Non-Orthogonal Multiple Access in LTE and 5G Networks », IEEE Commun. Mag., vol. 55, no 2, p. 185‑191, févr. 2017.

[5] M. Vaezi, Z. Ding, et H. V. Poor, Éd., Multiple Access Techniques for 5G Wireless Networks and Beyond. Cham: Springer International Publishing, 2019.

[6] A. E. Mostafa, Y. Zhou, et V. W. S. Wong, « Connection Density Maximization of Narrowband IoT Systems With NOMA », IEEE Trans. Wireless Commun., vol. 18, no 10, p. 4708‑4722, oct. 2019.

[7] Y. Yuan et al., « NOMA for Next-Generation Massive IoT: Performance Potential and Technology Directions », IEEE Commun. Mag., vol. 59, no 7, p. 115‑121, juill. 2021.

[8] M. B. Shahab, R. Abbas, M. Shirvanimoghaddam, et S. J. Johnson, « Grant-Free Non-Orthogonal Multiple Access for IoT: A Survey », IEEE Commun. Surv. Tutorials, vol. 22, no 3, p. 1805‑1838, 2020.

[9] F. A. Khales et G. A. Hodtani, « An evaluation of the coverage region for downlink Non-Orthogonal Multiple Access (NOMA) based on Power Allocation Factor », in 2017 Iran Workshop on Communication and Information Theory (IWCIT), Tehran, Iran, mai 2017, p. 1‑5.

[10] Q. C. Li, H. Niu, A. T. Papathanassiou, et G. Wu, « 5G Network Capacity: Key Elements and Technologies », IEEE Veh. Technol. Mag., vol. 9, no 1, p. 71‑78, mars 2014.

[11] X. Liang, X. Gong, Y. Wu, D. W. K. Ng, et T. Hong, « Analysis of Outage Probabilities for Cooperative NOMA Users with Imperfect CSI », in 2018 IEEE 4th Information Technology and Mechatronics Engineering Conference (ITOEC), Chongqing, China, déc. 2018, p. 1617‑1623.

[12] A. Agarwal, R. Chaurasiya, S. Rai, et A. K. Jagannatham, « Outage Probability Analysis for NOMA Downlink and Uplink Communication Systems With Generalized Fading Channels », IEEE Access, vol. 8, p. 220461‑220481, 2020.

[13] N. Tutunchi, A. Haghbin, et B. Mahboobi, « Complexity Reduction in Massive-MIMO-NOMA SIC Receiver in Presence of Imperfect CSI », Journal of Information Systems and Telecommunication (JIST), vol. 2, no 30, p. 113, août 2020.

[14] F. Kara et H. Kaya, « BER performances of downlink and uplink NOMA in the presence of SIC errors over fading channels », IET Communications, vol. 12, no 15, p. 1834‑1844, sept. 2018.

[15] C. A. Ramos-Arregu'n et al., « FPGA Open Architecture Design for a VGA Driver », Procedia Technology, vol. 3, p. 324‑333, 2012.

[16] « Zybo Z7 Reference Manual - Digilent Reference ». accessed on july 04, 2021. [Online]. available on: https://digilent.com/reference/programmable-logic/zybo-z7/reference-manual

[17] T. Tami, T. Messaoudene, A. Ferdjouni, et O. Benzineb, « Chaos secure communication' implementation in FPGA », in 2018 International Conference on Applied Smart Systems (ICASS), Medea, Algeria, nov. 2018, p. 1‑6.

[18] W. Tang, S. Yang, et X. Li, « Implementation of Space-time Coding and Decoding Algorithms for MIMO Communication System Based on DSP and FPGA », in 2019 IEEE International Conference on Signal Processing, Communications and Computing (ICSPCC), Dalian, China, sept. 2019, p. 1‑5.

[19] H. Sreenath et G. Narayanan, « FPGA Implementation of Pseudo Chaos-signal Generator for Secure Communication Systems », in 2018 International Conference on Advances in Computing, Communications and Informatics (ICACCI), Bangalore, sept. 2018, p. 804‑807.

[20] Q. Yingchao et Y. Feng, « Design and Implementation of Differential Frequency Hopping Communication System Based on FPGA », in 2018 IEEE 4th Information Technology and Mechatronics Engineering Conference (ITOEC), Chongqing, China, déc. 2018, p. 1006‑1010.

[21] M. A. Ahmed, K. F. Mahmmod, et M. M. Azeez, « On the performance of non-orthogonal multiple access (NOMA) using FPGA », IJECE, vol. 10, no 2, p. 2151, avr. 2020.

[22] M. Mekhfioui, A. Satif, O. Mouhib, R. Elgouri, A. Hadjoudja, et L. Hlou, « Hardware Implementation of Blind Source Separation Algorithm Using ZYBO Z7& Xilinx System Generator », in 2020 5th International Conference on Renewable Energies for Developing Countries (REDEC), Marrakech, Morocco, Morocco, juin 2020, p. 1‑5.

[23] T. Assaf, A. Al-Dweik, M. S. E. Moursi, H. Zeineldin, et M. Al-Jarrah, « NOMA Receiver Design for Delay-Sensitive Systems », IEEE Systems Journal, vol. 15, no 4, p. 5606‑5617.

[24] H. Semira et F. Kara, « Error Performance of Uplink SIMO-NOMA with Joint Maximum-Likelihood and Adaptive M-PSK », in 2021 IEEE International Black Sea Conference on Communications and Networking (BlackSeaCom), Bucharest, Romania, mai 2021, p. 1‑6.

[25] H. Semira, F. Kara, H. Kaya, et H. Yanikomeroglu, « Multi-User Joint Maximum-Likelihood Detection in Uplink NOMA-IoT Networks: Removing the Error Floor », IEEE Wireless Commun. Lett., vol. 10, no 11, p. 2459‑2463, nov. 2021.

[26] « Digital Modulation in FPGAs Xilinx using system generator (ASK, BPSK, FSK, OOK, QPSK) - File Exchange - MATLAB Central ». accessed on july 04, 2021. [online]. available on: https://www.mathworks.com/matlabcentral/fileexchange/14650-digital-modulation-in-fpgas-xilinx-using-system-generator-ask-bpsk-fsk-ook-qpsk?s_tid=FX_rc3_behav

[27] H. CJ, S. D. Hanwate, et A. S. Mali, « Hardware Implementation of BPSK System on Virtex2-Pro FPGA Using Xilinx System Generator », IRJES, vol2, issue1,p 18-24, jan 2013